JOURNAL OF VIROLOGY, Nov. 2005, p. 14371–14382 Vol. 79, No. 22
0022-538X/05/$08.00+0 doi:10.1128/JVI.79.22.14371–14382.2005

Role of Notch Signal Transduction in Kaposi's Sarcoma-Associated Herpesvirus Gene Expression

Heesoon Chang,[1] Dirk P. Dittmer,[2] Shin-Young Chul,[1] Youngkwon Hong,[3] and Jae U. Jung[1]*

Department of Microbiology and Molecular Genetics and Tumor Virology Division, New England Primate Research Center, Harvard Medical School, Southborough, Massachusetts 01772[1]; Department of Microbiology and Immunology and Lineberger Comprehensive Cancer Center, University of North Carolina at Chapel Hill, Chapel Hill, North Carolina 27599-7290[2]; and Cutaneous Biology Research Center, Massachusetts General Hospital, and Harvard Medical School, Charlestown, Massachusetts 02129[3]

Received 4 May 2005/Accepted 18 August 2005

Kaposi's sarcoma-associated herpesvirus (KSHV) RTA transcription factor is recruited to its responsive elements through interaction with a Notch-mediated transcription factor, RBP-Jκ, indicating that RTA mimics cellular Notch signal transduction to activate viral lytic gene expression. To test whether cellular Notch signal transduction and RTA are functionally exchangeable for viral gene expression, human Notch intracellular (hNIC) domain that constitutively activates RBP-Jκ transcription factor activity was expressed in KSHV-infected primary effusion lymphoma BCBL1 cells (TRExBCBL1-hNIC) in a tetracycline-inducible manner. Gene expression profiling showed that like RTA, hNIC robustly induced expression of a number of viral genes, including viral interleukin 6 (vIL-6), K3, and K5. Unlike RTA, however, hNIC was not capable of evoking the full repertoire of lytic viral gene expression and thereby lytic replication. To further understand the role of Notch signal transduction in KSHV gene expression, vIL-6 growth factor and K5 immune modulator genes were selected for detailed analysis. Despite the presence of multiple RBP-Jκ binding sites, hNIC targeted the specific RBP-Jκ binding sites of vIL-6 and K5 promoter regions to regulate their gene expression. These results indicate that cellular Notch signal transduction not only is partially exchangeable with RTA in regard to activation of viral lytic gene expression but also provides a novel expression profile of KSHV growth and immune deregulatory genes that is likely different from that of RTA-independent standard latency program as well as RTA-dependent lytic reproduction program.

Kaposi's sarcoma-associated herpesvirus (KSHV), also called human herpesvirus 8, is thought to be an etiologic agent of Kaposi's sarcoma (KS) (8). KSHV is also associated with two diseases of B-cell origin: primary effusion lymphoma and an immunoblast variant of Castleman disease (2, 5). An important step in the herpesvirus life cycle is the switch from latency to lytic replication. The KSHV replication and transcription activator (RTA) plays a central role in this switch. Ectopic expression of KSHV RTA is sufficient to disrupt viral latency and activate lytic replication to completion (22, 43, 57, 60). RTA activates the expression of numerous viral genes in the KSHV lytic cycle, including its own promoter, polyadenylated nuclear RNA, K12, ORF57, vOX-2, K14/vGPCR (viral G-protein-coupled receptor), and vIRF1. While the details of RTA-mediated transcriptional activation remain unclear, several pieces of evidence suggest that RTA activates its target promoter through direct binding to the specific sequence (40) and/or interaction with various cellular transcriptional factors. In fact, numerous cellular proteins, such as Stat3, KRBP, RBP-Jκ/CBF1, and CBP, interact with RTA, and these interactions synergize RTA transcriptional activity (24, 25, 37, 55, 64). Furthermore, our recent study demonstrated that RTA recruits cellular SWI/SNF and TRAP/Mediator complexes through its carboxy-terminal short acidic sequence. Recruitment of these complexes onto viral lytic promoters is essential for their effects on target promoters and thus for KSHV reactivation (23).

Epstein-Barr virus (EBV) EBNA2 and KSHV RTA have been shown to be recruited to their responsive elements through interaction with the transcription factor RBP-Jκ (29, 37, 41). RBP-Jκ binding sites are present in a number of EBNA2- and RTA-regulated viral promoters. RBP-Jκ, which was originally purified and characterized by Kawaichi et al. (34) and Hamaguchi et al. (26), is highly conserved in evolution from nematodes to humans. Biochemical and genetic studies have demonstrated that RBP-Jκ acts downstream of the receptor Notch. Activation of the Notch receptor by binding of its ligands (Delta, Jagged, or Serrate) leads to proteolytic cleavage of the receptor at the inner side of the membrane (52). The Notch intracellular domain (NIC) is then translocated to the nucleus, where it activates genes by interacting with RBP-Jκ. EBNA2 and RTA may thus be regarded as functional homologs or mimickers of the activated Notch protein. Indeed, NIC has been shown to be capable of functionally replacing EBNA2 in the context of EBV for primary B-cell transformation (21, 66). However, the cellular targets of cellular NIC do not completely overlap with those of EBNA2: both activate CD21 gene expression and repress immunoglobulin μ (Igμ) expression, whereas EBNA2, but not NIC, activates CD23a gene expression (59). Like EBV EBNA2, KSHV RTA strongly induces CD21 and CD23a expression through RBP-Jκ binding sites in the first intron of CD21 and in the CD23a core promoter, respectively (7). However, unlike EBV

* Corresponding author. Mailing address: Tumor Virology Division, New England Primate Research Center, Harvard Medical School, 1 Pine Hill Drive, Southborough, MA 01772. Phone: (508) 624-8083. Fax: (508) 786-1416. E-mail: jae_jung@hms.harvard.edu.

EBNA2, which alters Igμ and c-*myc* gene expression, RTA does not affect Igμ and c-*myc* expression, indicating that KSHV RTA targets the Notch signal transduction pathway in similar but distinct ways from those of EBV EBNA2. Furthermore, RBP-Jκ has been shown to be a critical component in mediating RTA activation of several KSHV target genes, including those for ORF57, thymidine kinase, and K14/vGPCR (37, 39). In fact, RBP-Jκ plays an essential role in RTA-mediated lytic reactivation of KSHV, since such reactivation is completely defective in RBP-Jκ$^{-/-}$ cells while being efficient in RBP-Jκ$^{+/+}$ cells (38). This indicates that RBP-Jκ plays an important role in the RTA-mediated lytic gene expression by directing RTA to viral target promoters through interaction.

The great puzzle of KSHV pathogenesis is that certain viral lytic genes either behave as oncogenes or at least have growth-promoting antiapoptotic or angiogenic properties (27). However, either these activities may be alleviated during the lytic replication cycle because cell growth is blocked by RTA-induced lytic replication. On the other hand, it is possible that cellular signal transduction, for example, the Notch signal pathway, may induce a unique expression profile of KSHV growth and immune deregulatory genes that is distinct from that of the latency program as well as the lytic program. In fact, the regulation of K14/vGPCR transcripts by RBP-Jκ suggests the possibility that Notch signaling is able to induce expression of this RNA outside the context of lytic KSHV replication (37, 39). Furthermore, this unique viral expression profile may ultimately lead to a favorable environment for viral persistent infection and pathogenesis. To test this hypothesis, we constructed KSHV-infected primary effusion lymphoma BCBL1 cells (TRExBCBL1-hNIC) expressing the constitutively active form of the human Notch intracellular (hNIC) domain in a tetracycline-inducible manner. It showed that hNIC specifically induced the expression of a number of KSHV genes, including K3, K5, and viral interleukin 6 (vIL-6). Particularly, hNIC-mediated activation of K5 gene expression conferred the downregulation of major histocompatibility complex class I (MHC-I) and CD54 surface expression. These results demonstrate that cellular hNIC induces the expression of a selected subset of KSHV genes, in particular growth and immune deregulatory genes, independently of RTA. Thus, as seen with EBV EBNA2, cellular Notch signal transduction is partially exchangeable with RTA in regard to activation of viral lytic gene expression but also provides a novel RTA-independent viral gene expression profile.

MATERIALS AND METHODS

Cell culture and transfection. 293T, BJAB, and BCBL-1 cells were grown in Dulbecco's modified Eagle's medium or RPMI 1640 medium supplemented with 10% fetal calf serum. OT11 (RBP-Jκ$^{-/-}$) and OT13 (RBP-Jκ$^{+/+}$) cells (kindly provided by T. Honjo, Kyoto University) were grown in Dulbecco's modified Eagle's medium supplemented with 10% fetal calf serum and 100 U/ml mouse gamma interferon.

Luciferase assay. Cells were transfected with pvIL6-Luc (kindly provided by Ren Sun, University of California, Los Angeles) or pK5-Luc, and β-galactosidase plasmid, and the indicated amount of empty vector or hNIC expression vector (kindly provided by P. Ling, Baylor College of Medicine) (21). At 48 h post-transfection, cells were washed twice with phosphate-buffered saline, lysed, and analyzed by luciferase assay (Promega, Madison, WI). Luciferase levels were normalized to β-galactosidase activity and presented as the increase in induction compared with the control.

Flow cytometry. Cells (5×10^5) were washed with RPMI 1640 medium containing 10% fetal calf serum and incubated for 30 min with antibodies. Cells were then incubated for 20 min at 4°C with secondary anti-mouse antibodies (Pharmingen, San Diego, CA). After each sample was washed, it was fixed with 2% paraformaldehyde, and fluorescence-activated cell sorting analysis was performed with a FACScan (Becton Dickinson, Mountainview, CA).

Real-time QPCR for KSHV. RNA was isolated as previously described (7) using RNAzol (Tel-Test, Inc., Friendswood, Texas). Poly(A) mRNA was prepared using dT beads (QIAGEN Inc., Valencia, CA) and reverse transcribed using Superscript II reverse transcriptase (Life Technologies, Rockville, MD) according to the manufacturer's recommendations. The procedures for real-time quantitative PCR (QPCR) analysis have been previously described (49, 58). The KSHV primers used in this analysis are available upon request from the authors. The final PCR contained 2.5 μl primer mix (final concentration, 166 nM), 7.5 μl 2× SYBR PCR mix (Applied Biosystems, Foster City, CA), and 5 μl sample. To guard against contamination and handling errors, all real-time QPCR mixtures were assembled in a segregated clean room using filtered pipette tips and a robot. Real-time PCR was performed using an ABI PRIZM 5700 machine (Applied Biosystems, Foster City, CA) and universal cycle conditions.

CHIP assay. Chromatin immunoprecipitation (CHIP) assay was performed according to the manufacturer's instructions (Upstate Biotech) with several modifications. Briefly, culture dishes were treated with 1% formaldehyde for 10 min at room temperature. After a brief sonication, immunoprecipitation was performed using the appropriate antibody. After several washings, the immunocomplexes were eluted with 50 mM Tris, pH 8.0, 1 mM EDTA, and 1% sodium dodecyl sulfate at 65°C for 10 min, adjusted to 200 mM NaCl, and incubated at 65°C for 5 h to reverse the cross-links. After successive treatments with 10 μg/ml RNase A and 20 μg/ml proteinase K, the samples were extracted with phenol-chloroform and precipitated with ethanol. One-tenth of the immunoprecipitated DNAs was analyzed by PCR with the primer sets for R1 (5′ primer, GGTAAG CATATAAGGAACTCGGCG; 3′ primer, AGCTATTAGGCGTGTACGACA CGA), R2/3 (5′ primer, TAATAGCTGCTGCTACGGGTTCCA; 3′ primer, TTGGGCCGCAGTGATATCTTCAAC), R4 (5′ primer, AACTGCTCGAGG CGACAACGCCAT; 3′ primer, GGACACGCGTCATCACTAGTTATG), R5 (5′ primer, CCCTTATTTCATAGGTCCGGTGTG; 3′ primer, ACAACCCAC CCTGCTTTAGCTCTA), and R6 (5′ primer, GACAGTTTTCCAGGGAAAG CCTGG; 3′ primer, TGCAGCTGGGGTGGAAGTCTGAAA). Amplifications (26 cycles) were performed with an MJ thermal cycler, and the PCR products were analyzed in 3% polyacrylamide gels.

RESULTS

Tetracycline-inducible expression of hNIC in BJAB and BCBL1 cells. To test whether Notch signaling affected KSHV gene expression, the intracellular cytoplasmic region of human Notch receptor (hNIC), which induces the constitutive activation of RBP-Jκ-mediated transcription (42), was expressed in KSHV-infected BCBL1 cells in a tetracycline-inducible manner as previously described (47). These cells were designated TRExBCBL1-hNIC. KSHV-negative BJAB cells (TRExBJAB-hNIC) expressing hNIC in a tetracycline-inducible manner were also constructed as controls. Immunoblot assay showed that treatment of these cells with doxycycline (doxy) rapidly induced hNIC expression (Fig. 1A). As previously shown (7), RTA also effectively induced the upregulation of CD21 and CD23 surface expression and downregulation of MHC-I and CD54 surface expression on BCBL1 cells (7, 62) (Fig. 1B). To examine the effect of hNIC on lymphocyte antigen expression, TRExBCBL1-cDNA5 control cells and TRExBCBL1-hNIC cells were tested for CD21, CD23, MHC-I, and MHC-II surface expression upon doxy treatment for 0, 24, and 48 h. It showed that hNIC considerably downregulated MHC-I surface expression on TRExBCBL-1 cells, whereas it did not affect CD21, CD23, and MHC-II surface expression (Fig. 1B and data not shown). In contrast, hNIC expression has been shown to have no effect on MHC-I surface expression on TRExBJAB-hNIC cells (7). This indicates that hNIC specifically downregu-

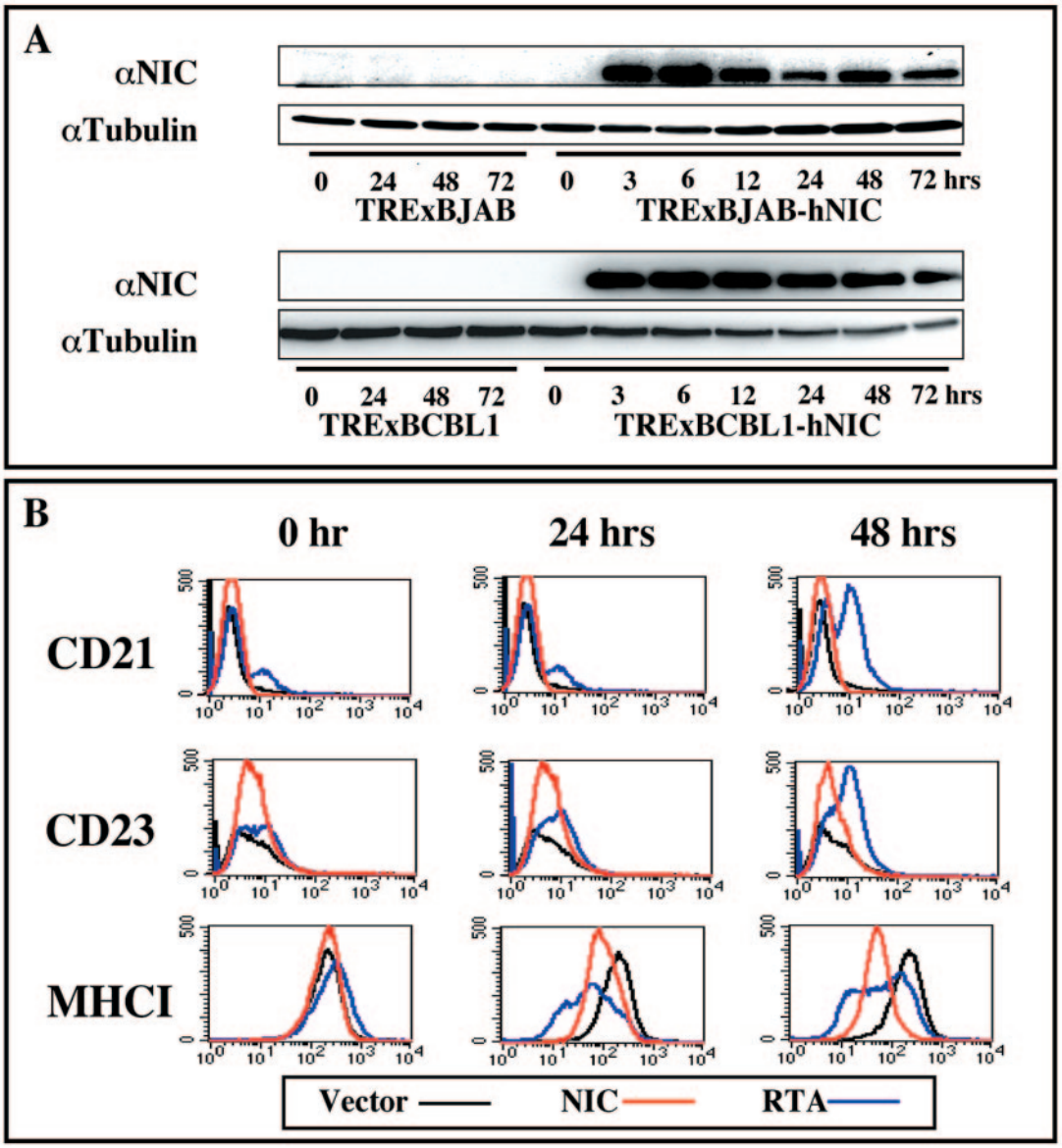

FIG. 1. Induction of hNIC expression and MHC-I downregulation. (A) Induction of hNIC expression. TREXBJAB-cDNA5, TREXBJAB-hNIC, TREXBCBL1-cDNA5, and TREXBCBL1-hNIC cells were stimulated with or without 1 μg/ml doxy for 0, 24, 48 or 72 h. Whole-cell lysates were used for immunoblotting with anti-Flag (αNIC) and antitubulin (αTubulin) antibodies. (B) Downregulation of MHC-I surface expression. TREXBCBL1-cDNA5 (black lines), TREXBCBL1-hNIC (red lines), and TREXBCBL1-RTA (blue lines) cells were treated with 1 μg/ml doxy for 0, 24, and 48 h, fixed, and then reacted with the indicated antibodies for flow cytometry.

lates MHC-I surface expression on KSHV-infected BCBL1 cells, but not on uninfected BJAB cells.

Induction of K3 and K5 expression by hNIC. Tetracycline-inducible expression of KSHV RTA in BCBL1 cells induces K3 and K5 expression, which leads to the drastic downregulation of MHC-I and CD54 surface expression (7). Because of their functional similarity, we compared the effect of hNIC on lymphocyte surface antigen expression with that of RTA. TREXBCBL1-cDNA5, TREXBCBL1-hNIC, and TREXBCBL1-RTA cells were treated with doxy for 0, 24, 48, and 72 h and tested for expression of various surface antigens, including MHC-I, MHC-II, and CD54. KSHV K8.1 envelope protein was also included as a means to determine lytic replication. It showed that hNIC expression induced the strong downregulation of MHC-I and CD54 on TREXBCBL1 cells at levels equivalent to those induced by RTA expression (Fig. 2). However, unlike TREXBCBL1-RTA cells on which the surface expression of K8.1 viral envelope protein increased upon RTA expression, TREXBCBL1-hNIC cells displayed no detectable increase of K8.1 surface expression upon hNIC expression (Fig. 2). Since KSHV K3 and K5 efficiently downregulated MHC-I and CD54 surface expression (11, 12, 31, 32, 50), we tested whether hNIC affected viral protein expression, specifically K3 and K5. Immunoblotting assay with various KSHV antibodies showed that hNIC induced K3, K5, and vIL-6 protein levels but not K8.1 and LANA protein levels (Fig. 3). These results

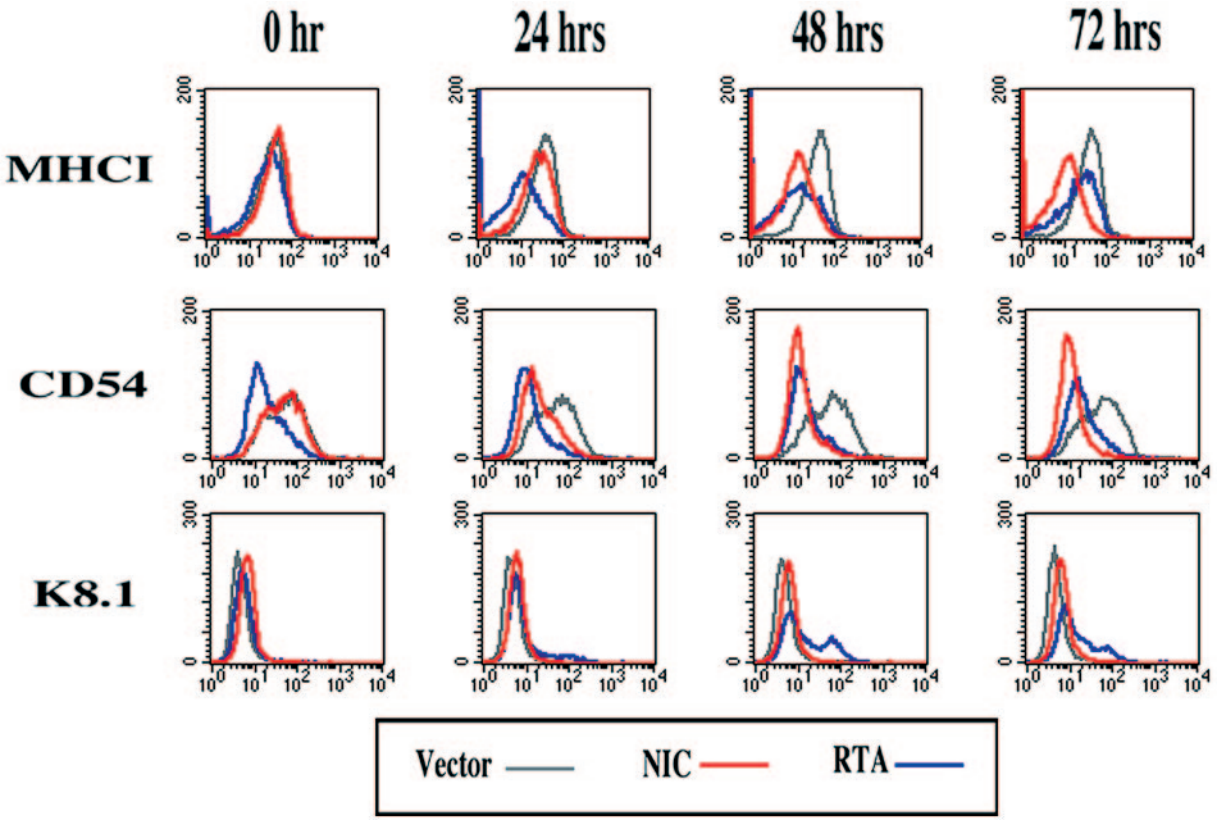

FIG. 2. MHC-I and CD54 surface expression. TRExBCBL1-cDNA5, TRExBCBL1-hNIC, and TRExBCBL1-RTA cells were treated with 1 μg/ml doxy for 0, 24, 48 h, and 72 h, fixed, and then reacted with antibodies indicated to the left of the figure for flow cytometry. Gray lines indicate control TRExBCBL1-cDNA5 cells, red lines indicate TRExBCBL1-hNIC cells, and blue lines indicate TRExBCBL1-RTA cells.

showed that hNIC efficiently induced K3, K5, and vIL-6 expression independently of RTA, which likely led to downregulation of MHC-I and CD54 surface expression. However, unlike RTA that efficiently induced K8.1 envelope expression, hNIC did not affect K8.1 envelope protein expression under the same conditions (Fig. 2 and 3).

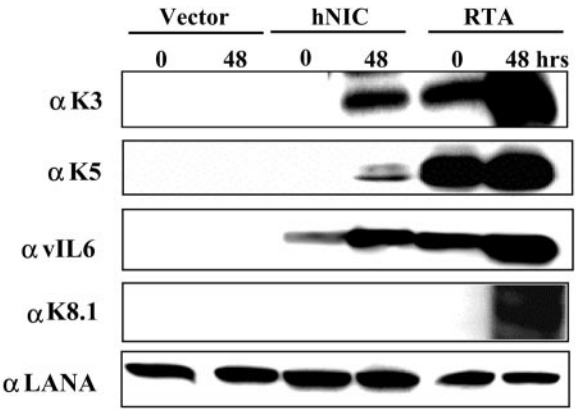

FIG. 3. Induction of K3, K5, and vIL-6 expression by hNIC. TRExBCBL1-cDNA5 (Vector), TRExBCBL1-hNIC (hNIC), and TRExBCBL1-RTA (RTA) cells were treated with 1 μg/ml doxy for 0 and 48 h. Whole-cell lysates were used for immunoblotting with antibodies specific for K3, K5, vIL-6, K8.1, and LANA as indicated to the left of the figure. These results were reproduced on at least two independent occasions.

Genome-wide effects of hNIC on KSHV gene expression. In order to evaluate the impact of hNIC on the KSHV life cycle, we analyzed whether hNIC expression affected KSHV gene expression in latently infected BCBL-1 cells. Approximately 1×10^7 TRExBCBL1-cDNA5 cells and TRExBCBL1-hNIC cells were treated with doxy for 0, 24, and 48 h, and mRNAs were isolated, reverse transcribed, and analyzed using our previously developed real-time quantitative reverse transcription-PCR array for KSHV (17, 20). Hierarchical clustering was performed with KSHV genes only, not on the samples, which were a time series. Clustering was based on a standard correlation metric. A detailed validation of these methods of analysis for viral arrays has been published recently (18). Figure 4 shows the tree view representation after hierarchical clustering of glyceraldehyde-3-phosphate dehydrogenase-normalized relative expression levels (dCT) of KSHV viral mRNAs. It showed that hNIC expression efficiently induced expression of a subset of KSHV genes, including vIL-6, K3, K4, K5, K7, PAN, Orf4, Orf11, Orf17, Orf23, Orf32, Orf35, Orf37, Orf38, Orf39, Orf46, Orf48, Orf49, Orf52, Orf53, Orf55, Orf57, Orf66, Orf70, and Orf75 (Fig. 4). Particularly, the induction kinetics of K5, K7, and Orf11 mRNAs were faster than those of other viral genes upon doxy treatment (Fig. 4). In addition, the low levels of K5, Orf11, and K7 were also detected in

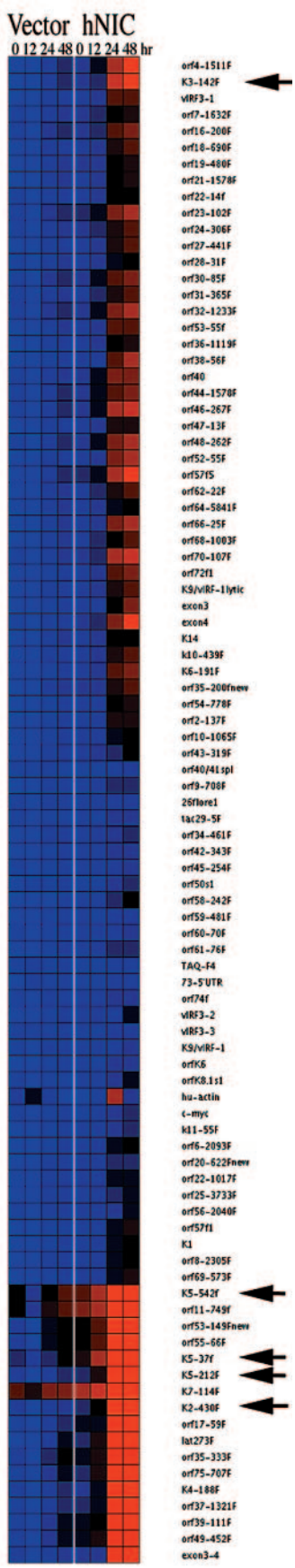

TRExBCBL1-NIC cell expression before doxy treatment, which was likely derived from the leakiness of tetracycline-inducible NIC expression (Fig. 4). These results showed that Notch signaling induced expression of a selected subset of KSHV genes. However, unlike RTA, hNIC was not capable of evoking the full repertoire of lytic viral gene expression and thereby lytic replication.

Increase of vIL-6 promoter activity by hNIC. Notch signal transduction has been shown to modulate cellular growth factor expression, which regulates growth control and differentiation (42, 44, 53). In order to delineate the effect of Notch-mediated activation on KSHV gene expression and pathogenesis, the vIL-6 gene promoter was selected for further analysis. The previous study has defined the RTA-responsive element to the 48-bp region spanning between −462 and −414 from the vIL-6 translational initiation site (14). The upstream sequence of the vIL-6 promoter region was cloned into pGL3-basic to derive luciferase reporter pvIL-6(−507) plasmid (the numbers in parentheses indicate the lengths of the upstream region from the vIL-6 translation initiation site). Reporter plasmids were transfected into BJAB B cells and 293T epithelial cells together with either pcDNA5/hNIC or vector pcDNA5. Plasmid pGK-βGal that contains the coding sequence for β-galactosidase under the control of a constitutively active promoter was included as an internal control for transfection efficiency. Cell extracts were harvested and assayed for both luciferase and β-galactosidase activities at 48 h posttransfection. It showed that pvIL-6(−507) was activated 22- and 16-fold by hNIC expression in BJAB and 293T cells, respectively, indicating that the 507-nucleotide sequence upstream of the vIL-6 open reading frame is sufficient to respond to hNIC-mediated activation (Fig. 5). Precise inspection reveals that the vIL-6 promoter region contains two potential RBP-Jκ binding sites (GTGGGAA), R1 (GCGGGAA) and R2 (GTGGGGA) (Fig. 5). To further identify the specific sequence of the vIL-6 promoter responsible for hNIC-mediated activation, we generated additional luciferase reporter constructs containing deletions and/or point mutations (Fig. 5). These reporter plasmids were cotransfected with pcDNA5/hNIC or pcDNA5 into BJAB or 293T cells as described above. As shown in Fig. 5, when the sequence between −507 and −412 was deleted, the reporter response to hNIC was affected at a minimal level. However, when the sequence between −507 and −336 was deleted, the reporter response to hNIC was drastically reduced (Fig. 5). Furthermore, luciferase assays with pvIL-6(-m507R1), pvIL-6(-m507R2), pvIL-6(-m507R1/2), and pvIL-6(-m412) point mutants showed that mu-

FIG. 4. Genome-wide effects of hNIC on KSHV gene expression. "Heat map" representation of KSHV mRNA upon hNIC expression was determined by real-time quantitative reverse transcription-PCR. The values were normalized to glyceraldehyde-3-phosphate dehydrogenase mRNA levels, and the medians were centered. They were clustered on the basis of a Euclidean metric and were represented on a logarithm 2 scale, to allow for a more robust statistical analysis. Black represents the decreased level and red represents the increased level relative to the median (blue) across all time points for both conditions ($n = 8$). Vector-expressing BCBL1 cells (Vector) and hNIC-expressing BCBL1 cells (hNIC) were examined. Arrows indicate KSHV K3, K5, and vIL-6 (K2) genes.

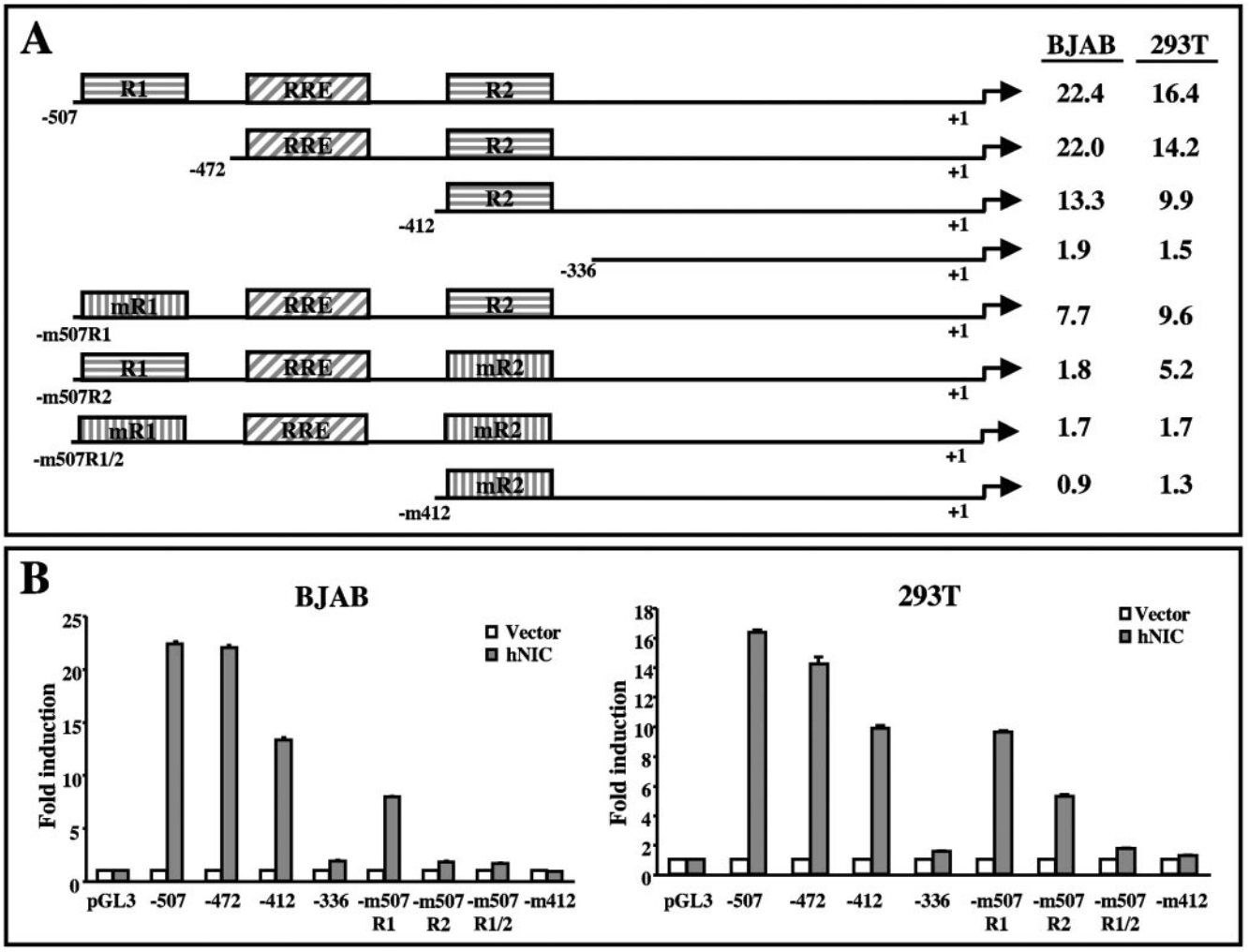

FIG. 5. Activation of vIL-6 expression induced by hNIC. (A) Schematic diagrams of the potential RBP-Jκ binding sites within the vIL-6 promoter region. The positions of the two putative RBP-Jκ binding sequences (R1 and R2), the mutations at the RBP-Jκ binding sequences (mR1 and mR2), and the RTA-responsive elements (RRE) are shown. The numbers below the maps indicate the position relative to the translational start site (+1). The numbers to the right of the figure indicate the increase in induction in BJAB and 293T cells upon hNIC expression over the control vector expression. (B) Luciferase assay. Wild-type (pGL3) or mutant vIL-6 promoter luciferase reporter together with the pGK-β-gal construct was transfected into BJAB or 293T cells with pcDNA5 vector (Vector) or pDNA5-hNIC (hNIC). The mutant vIL-6 promoter luciferase reporters used were pvIL-6(−507), pvIL-6(−472), pvIL-6(−412), pvIL-6(-m507R1), pvIL-6(-m507R2), pvIL-6(-m507R1/2), and pvIL-6(-m412) (only the last part of the plasmid designation is shown in the figure). At 48 h posttransfection, cell lysates were used for reporter assays. Luciferase activity is presented as the average of three independent experiments.

tation at the R2 site significantly abrogated the hNIC-mediated activation of vIL-6 promoter activity (Fig. 5). These results indicate that the R2 RBP-Jκ binding site of vIL-6 promoter is primarily responsible for hNIC-mediated activation.

We next asked whether RBP-Jκ was necessary for the hNIC-mediated activation of vIL-6 promoter activity. RBP-Jκ$^{-/-}$ knockout (OT11) and its revertant RBP-Jκ$^{+/+}$ (OT13) mouse embryonic fibroblast (MEFs) were transfected with various luciferase constructs containing the wild-type or mutant sequence of the vIL-6 promoter region together with pcDNA5/hNIC or pcDNA5. This showed a near-total loss of the hNIC-mediated activation of vIL-6 promoter activity in RBP-Jκ$^{-/-}$ OT11 cells (Fig. 6). In contrast, pvIL-6(−507), pvIL-6(−472), and pvIL-6(−412) promoter constructs that contained the R2 RBP-Jκ site remained active upon hNIC expression in RBP-Jκ$^{+/+}$ OT13 cells, whereas the pvIL-6(-m412) mutant construct with the R2 site deleted showed no activation under the same conditions (Fig. 6). Finally, RBP-Jκ dominant-negative mutant that contained a defect in DNA binding ability (61) was transfected into 293T cells together with hNIC and vIL-6 promoter constructs. This showed that the introduction of the RBP-Jκ dominant-negative mutant dramatically suppressed the hNIC-mediated activation of vIL-6 promoter activity (Fig. 6, bottom). These results demonstrate that the hNIC-mediated activation of vIL-6 promoter activity requires a functionally active RBP-Jκ factor and that the R2 RBP-Jκ binding sequence of the vIL-6 promoter region likely plays an important role in hNIC-mediated gene expression.

Increase of K5 promoter activity by hNIC. To further delineate the effect of hNIC on K5 expression, we constructed

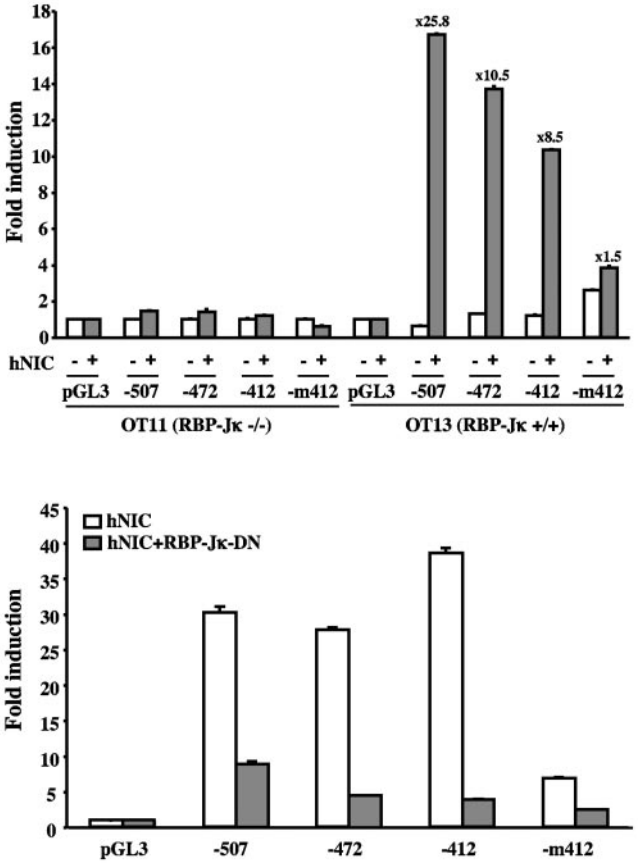

FIG. 6. Role of RBP-Jκ in the hNIC-mediated activation of vIL-6 promoter activity. (Top) hNIC-mediated activation of vIL-6 requires RBP-Jκ expression. RBP-Jκ$^{-/-}$ OT11 and RBP-Jκ$^{+/+}$ OT13 MEFs were transfected with vIL-6 promoter luciferase reporters and pGK-β-gal together with pcDNA5 vector or pDNA5-hNIC. The mutant vIL-6 promoter luciferase reporters used were pvIL-6(−507), pvIL-6(−472), pvIL-6(−412), and pvIL-6(-m412) (only the last part of the plasmid designation is shown in the figure). At 48 h posttransfection, cell lysates were used for reporter assays. Luciferase activity is presented as the average of three independent experiments. (Bottom) Inhibition of the hNIC-induced activation of vIL-6 promoter activity by RBP-Jκ dominant-negative (DN) mutant. Wild-type (pGL3) or mutant vIL-6 promoter luciferase reporter together with pGK-β-gal was transfected into 293T cells with pDNA5-hNIC alone or with pcDNA5-hNIC and pcDNA5-RBP-Jκ DN vectors. At 48 h posttransfection, cell lysates were used for reporter assays. Luciferase activity is presented as the average of three independent experiments.

luciferase reporters containing the K5 promoter region. On the basis of the presence of six potential RBP-Jκ binding sequences within 1 kb of sequence upstream of the ATG codon of the K5 gene, we constructed serial deletions from the 5′ ends of the constructs [pK5(−1042), pK5(−952), pK5(−781), pK5(−496), and pK5(−232)] and examined their responses to hNIC expression (Fig. 7A). In addition, pK5(-m781) contained the replacement of R3 (AAGGGTC) and R4 (CTGGGAA) sequences with mR3 (CCTTTGA) and mR4 (AGTTTCC) sequences, respectively, and both pK5(-m1042) and pK5(-m496) contained the replacement of R5 (AACGCTT) sequence with mR5 (CCATAGG) sequence (Fig. 7A). Interestingly, pK5(−496) promoter activity showed the maximum increase (10.5-fold in 293T cells and 4.2-fold in BJAB cells) upon hNIC expression over control vector expression, whereas other pK5 reporters showed significantly reduced levels of activation (1.5- to 2.7-fold) under the same conditions (Fig. 7). Furthermore, the pK5(-m781) construct that contained the mutations at the R3 and R4 sequences remained active upon hNIC expression, whereas the pK5(-m496) construct that contained the mutation at the R5 sequence no longer responded to hNIC expression (Fig. 7). Finally, pK5(m-1042) that contained all other RBP-Jκ binding sites with the mutated R5 showed no activation upon NIC expression (Fig. 7). These results indicate that the R5 RBP-Jκ binding sequence between −496 and −232 of the K5 promoter region is the primary target for hNIC action. Furthermore, the K5 promoter sequence upstream of −496 bp may contribute to the negative effect on K5 expression.

To further detail the activation of the K5 promoter induced by hNIC, OT11 RBP-Jκ$^{-/-}$ and OT13 RBP-Jκ$^{+/+}$ MEFs were transfected with various luciferase constructs containing the wild-type or mutant sequence of the K5 promoter region together with pcDNA5/hNIC or pcDNA5. This revealed that as seen with the vIL-6 promoter (Fig. 6), a near-total loss of the hNIC-mediated activation of K5 promoter activity was observed in OT11 RBP-Jκ$^{-/-}$ cells (Fig. 8A). In contrast, pK5(−496) promoter constructs showed a maximum level of activation induced by hNIC in RBP-Jκ$^{+/+}$ OT13 cells, whereas pK5(−1042), pK5(−781), and pK5(-m496) promoter constructs showed a minimal level of activation under the same conditions (Fig. 8A). Finally, as seen with the vIL-6 promoter (Fig. 6), introduction of RBP-Jκ dominant-negative mutant dramatically abrogated the hNIC-mediated activation of K5 promoter activity, in particular pK5(−496) promoter activity (Fig. 8B). These results demonstrate that the hNIC-mediated activation of K5 promoter activity requires a functionally active RBP-Jκ and that the R5 RBP-Jκ binding sequence of the K5 promoter region likely plays a major role in hNIC-mediated activation.

To further confirm the primary role of the R5 RBP-Jκ binding sequence in hNIC-mediated activation, chromatin immunoprecipitation assay was used to examine the amount of hNIC protein recruited onto the RBP-Jκ binding sequences of K5 promoters. 293T cells were transfected with pGL3 or pK5(−1042) reporter together with the Flag-tagged hNIC expression vector. Untransfected 293T cells were also included as controls. At 48 h posttransfection, cell lysates were used for immunoprecipitation with an anti-Flag antibody or without antibody. Immune complexes were then used for PCR analysis with primers specific for each RBP-Jκ binding sequence. It showed that the Flag-tagged hNIC was efficiently recruited onto the R5 RBP-Jκ binding sequence, whereas other RBP-Jκ binding sequences showed no detectable level of hNIC recruitment (Fig. 8C). This indicates that the activation of K5 promoter activity is most likely mediated by the efficient recruitment of hNIC onto the R5 RBP-Jκ binding sequence.

DISCUSSION

RBP-Jκ is a downstream transcription factor of the Notch pathway that is important in development and cell fate determination (44, 45, 53). The intracellular domain of activated Notch receptor is released from the plasma membrane through proteolytic cleavage and is translocated to the nucleus, where

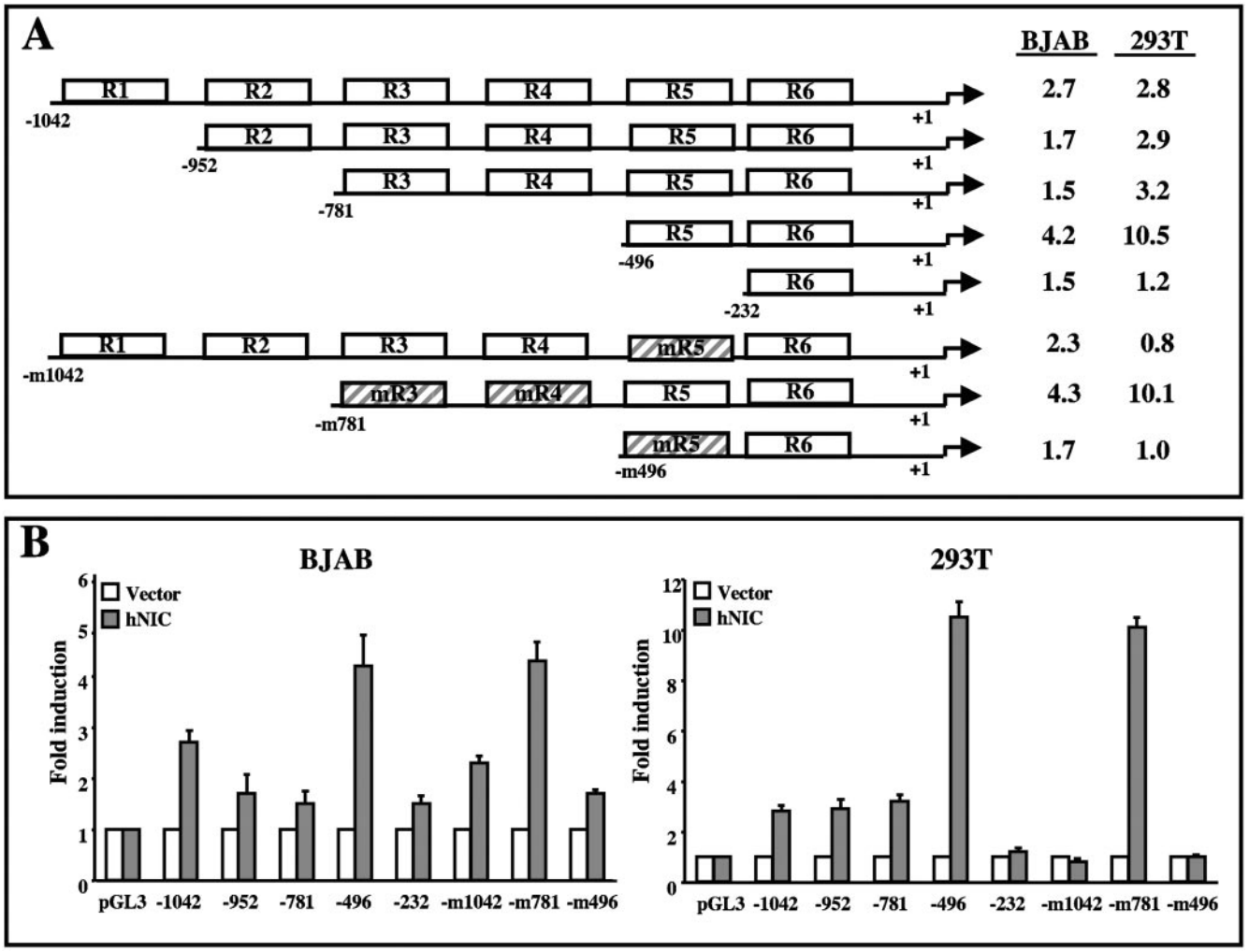

FIG. 7. Activation of K5 expression induced by hNIC. (A) Schematic diagrams of the potential RBP-Jκ binding sites within the K5 promoter region. The six putative RBP-Jκ binding (GTGG/AGAA) sequences (white R1 to R6 boxes) and mutants (hatched mR3 to mR5 boxes) are indicated. Numbers indicate the position relative to the translational start site (+1). The numbers to the right of the figure indicate the increase in induction in BJAB and 293T cells upon hNIC expression over control vector expression. (B) Luciferase assay. Wild-type (pGL3) or mutant K5 promoter luciferase reporter together with pGK-β-gal construct was transfected into BJAB or 293T cells with pcDNA5 vector or pcDNA5-hNIC. The mutant K5 promoter luciferase reporters used were pK5(−1042), pK5(−952), pK5(−781), pK5(−496), pK5(−232), pK5(-m1042), pK5(-m781), and pK5(-m496) (only the last part of the plasmid designation is shown in the figure). At 48 h posttransfection, cell lysates were used for reporter assays. Luciferase activity is presented as the average of three independent experiments.

it is directed to target promoters through RBP-Jκ interaction (42). A previous report (37) has shown that the KSHV RTA protein mimics cellular Notch signal transduction by interacting with RBP-Jκ and by activating RBP-Jκ-dependent activation of viral lytic gene expression. Here, we also demonstrate that the constitutively active form of the human Notch signaling molecule, hNIC, is partially exchangeable with RTA in viral lytic gene expression. A microarray showed that hNIC robustly induced expression of a number of viral genes, including vIL-6, K3, and K5, but was not capable of evoking the full repertoire of lytic viral gene expression. Further detailed analysis showed that hNIC targeted the specific RBP-Jκ binding sites of vIL-6 and K5 promoter regions to induce their gene expression. These results indicate that cellular Notch signal transduction not only is partially exchangeable with RTA in regard to activation of viral lytic gene expression but also provides a novel expression profile of KSHV growth and immune deregulatory genes.

RTA transcription factor that controls the switch from latency to lytic replication interacts with RBP-Jκ to activate viral gene expression. The fact that many KSHV lytic genes, including RTA itself, contain RBP-Jκ binding sites has raised the possibility that RTA/RBP-Jκ-mediated gene expression may be central to the switch from latency to lytic replication (7, 37, 39). EBV EBNA2 has also been shown to be recruited to its responsive elements through interaction with RBP-Jκ (29, 37, 41), indicating that EBNA2 and RTA may thus be regarded as functional homologs or mimickers of the activated Notch protein. Indeed, hNIC has been shown to be capable of functionally replacing EBNA2 in the context of EBV for primary B-cell transformation (21). We also showed that hNIC was capable of partially replacing the RTA function in KSHV gene expres-

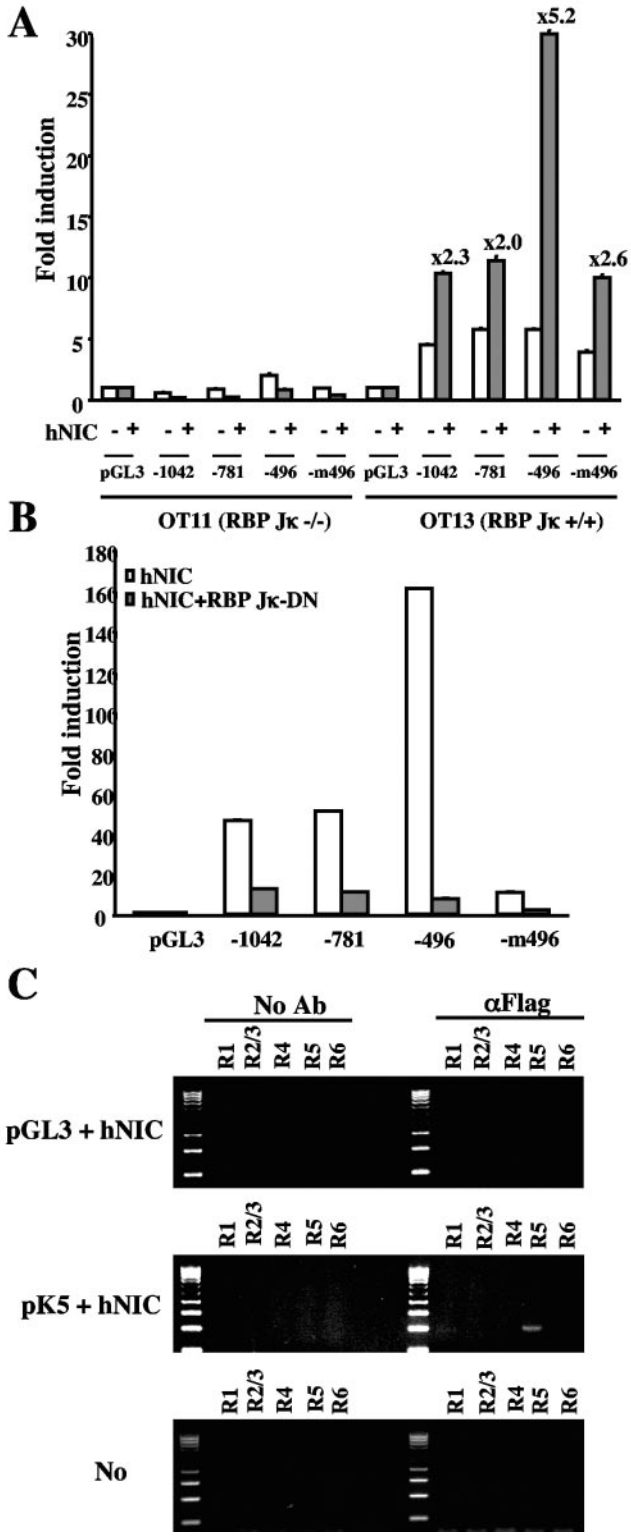

FIG. 8. Role of RBP-Jκ in the hNIC-mediated activation of K5 promoter activity. (A) hNIC-mediated activation of K5 requires RBP-Jκ expression. RBP-Jκ$^{-/-}$ OT11 and RBP-Jκ$^{+/+}$ OT13 MEFs were transfected with K5 promoter luciferase reporters and pGK-β-gal together with pcDNA5 vector or pDNA5-hNIC. The K5 promoter luciferase reporters used pK5(−1042), pK5(−781), pK5(−496), pK5(−232), and pK5(-m496) (only the last part of the plasmid designation is shown in the figure). At 48 h posttransfection, cell lysates were used for reporter assays. Luciferase activity is presented as the average of three independent experiments. (B) Inhibition of the hNIC-induced activation of K5 promoter activity by RBP-Jκ dominant-negative (DN) mutant. Wild-type (pGL3) or mutant K5 promoter luciferase reporter together with pGK-β-gal was transfected into 293T cells with pDNA5-hNIC alone or with pcDNA5-hNIC and pcDNA5-RBP-Jκ DN vectors. At 48 h posttransfection, cell lysates were used for reporter assays. Luciferase activity is presented as the average of three independent experiments. (C) CHIP assay. 293T cells were transfected with pGL3 and pcDNA5-hNIC or pK5(−1042) and pcDNA5-hNIC or not transfected with DNA (No). At 48 h posttransfection, cell lysates were used for immunoprecipitation with an anti-Flag antibody (αFlag) or without antibody (No Ab). Then, immune complexes were used for PCR analysis with primers to specifically amply the R1, R2/3, R4, R5, and R6 RBP-Jκ binding sequences. PCR products were separated by 3% agarose gel electrophoresis.

sion. Interestingly, while hNIC induced the expression of approximately 24 KSHV genes and RTA contained the functional RBP-Jκ binding site in its promoter region, RTA was not one of the genes induced by hNIC. A recent study has demonstrated that RBP-Jκ binding sites within the RTA promoter are critical for the repression rather than the activation of its expression (36). Specifically, LANA physically associates with RBP-Jκ, and this interaction represses RTA expression by targeting this complex to the RBP-Jκ binding sites within its promoter, which ultimately leads to the maintenance of KSHV latency (36). Thus, RBP-Jκ binding sites in viral promoters provide positive or negative effects on their gene expression, which is likely dependent on the interaction with target transcriptional factors. Nevertheless, these results indicate that hNIC-mediated activation of KSHV gene expression is specific and RTA independent.

Our previous report (7) demonstrated that KSHV RTA induces both CD21 and CD23a surface expression on BJAB cells, whereas cellular NIC induces only CD21 surface expression on BJAB cells. However, NIC expression was not capable of inducing CD21 surface expression on KSHV-infected BCBL1 cells. This is likely because the origin of primary effusion lymphoma (PEL) cells is different from that of BJAB cells. BAJB cells that are derived from mature B cells show the surface expression of CD19, CD20, and CD21 mature B-cell markers (56). In contrast, PEL cells that carry plasma cell types do not express any of mature B-cell markers, including CD19, CD20, and CD21 (6). Since NIC expression was not capable of inducing CD21 surface expression on PEL cells, this indicates that cellular transcription factors other than Notch-mediated RBP-Jκ activity are necessary for CD21 gene expression.

Despite the broad effect of hNIC on KSHV gene expression, hNIC was not capable of inducing the complete cycle of viral lytic replication, suggesting that a number of other cellular partners are required for RTA to evoke the full repertoire of lytic viral gene expression and thereby lytic replication. In fact, Liang and Ganem (39) have also discussed as unpublished results that ectopic expression of the Notch intracellular domain or EBNA2 fails to induce KSHV lytic replication. The previous and current studies suggest that activation through the RBP-Jκ-mediated signal transduction is necessary for lytic induction but not sufficient for the completion of lytic replication. Interestingly, K5 and Orf11 genes showed the faster kinetics of expression upon hNIC expression compared to the

rest of other viral genes, suggesting that they may be the initial targets for Notch signal transduction. Precise inspection reveals the potential six RBP-Jκ binding sites in the K5 promoter region. A series of mutational analysis indicated the complexity of transcriptional regulation of the K5 promoter. First, the R5 RBP-Jκ binding site within the K5 promoter likely played the major role in the hNIC-mediated activation. CHIP assay of K5 promoter and reporter assay with RBJ-Jκ dominant-negative mutant further supported this notion. However, the deletion mutations of the first four (R1, R2, R3, and R4) RBP-Jκ sites enhanced K5 promoter activity in both BJAB B cells and 293T epithelial cells, indicating that they might influence K5 promoter activity in a repressive way. These results were also supported by the study of RBP-Jκ-null murine fibroblasts. RBP-Jκ is a repressor in the ground state without upstream signal transduction, whereas upon stimulation its interaction with the Notch intracellular domain then relieves this repression and turns on target genes. This suggests that RBP-Jκ may initially target the first four R1, R2, R3, and R4 sites to repress K5 promoter activity and to keep the ground status in the absence of upstream Notch signaling. Upon stimulation, Notch intracellular domain is then recruited to the R5 site through RBP-Jκ interaction to evoke K5 promoter activation. This indicates that RBP-Jκ is an important transcription factor that regulates K5 gene expression in both positive and negative ways.

Tomescu et al. (62) have described the surface downregulation of MHC-I, CD31, and CD54 immunoregulatory proteins by KSHV in newly infected endothelial cells. Analysis of viral mRNA expression both in vivo within Kaposi's sarcoma lesions and in vitro in infected PEL and endothelial cells indicates that KSHV gene expression is restricted to a small subset of latent genes (3, 4, 9, 10, 15–17, 20, 33, 35, 46, 62, 65). While KSHV lytic protein K3 and K5 are capable of downregulating MHC-I and/or CD54, their contribution to immune evasion by KSHV during latency is less clear. We showed that Notch signal transduction induced K5 expression independent of RTA. This result may relate to the previous finding that K5 protein is detected in KSHV latently infected KS lesion (48). It is possible that K5 may be expressed at a low level in latently infected cells, which is sufficient to induce surface molecule downregulation. In addition, under this condition, K5 expression is likely independent of the lytic transcription factor RTA but dependent on the Notch signal-mediated RBP-Jκ transcription factor. In fact, we found that KSHV-infected BCBL1 cells likely displayed the constitutive activation of ligand-mediated Notch signal transduction, evidenced by the expression of Jagged and the complete proteolytic process of Notch receptors (unpublished results). Furthermore, a recent report has shown that KSHV-infected cells have elevated not only the level of activated Notch and but also the activated level of Notch-mediated transcription activity (13). Furthermore, inhibitors that block Notch activation resulted in apoptosis in primary and immortalized KS cells. The results suggest that targeting Notch signaling may be of therapeutic value in KS patients.

RBP-Jκ is a transcription factor whose function switches from a repressor in the ground state to an activator upon interaction with the Notch intracellular domain, which relieves its repression activity and then gains its activation activity to turn on target genes. Because of its important roles in a variety of cells, RBP-Jκ has been shown to be a common target for viruses, particularly gammaherpesviruses, which scrounge the Notch signaling pathway. Examples are KSHV RTA and LANA (36), murine gammaherpesvirus 68 RTA (51), and EBV EBNA2 and EBNA3 (21, 30, 54, 59). In all cases, these viral transcription factors interact with RBP-Jκ and this interaction activates target gene expression. Furthermore, the Notch pathway has also been reported to play a role in the pathogenesis of adenovirus (19), simian virus 40 (1), and human papillomavirus (28, 63). Here, we demonstrate that cellular Notch signal transduction not only is partially exchangeable with RTA in regard to activation of viral lytic gene expression but also provides a novel expression profile of KSHV growth and immune deregulatory genes. With all these activities of Notch signal transduction in mind, further study of Notch signal transduction should be informative for elucidation of the mechanisms of immune evasion and pathogenesis associated with KSHV latency.

ACKNOWLEDGMENTS

We especially thank R. Sun, P. Ling, and D. Hayward for providing constructs and T. Honjo for providing OT13 and OT11 cells.

This work was partly supported by U.S. Public Health Service grants CA115284, CA86841, CA91819 (J. U. Jung), CA109232 (D. P. Dittmer) and RR00168. J. Jung is a Leukemia & Lymphoma Society Scholar.

REFERENCES

1. **Bocchetta, M., L. Miele, H. I. Pass, and M. Carbone.** 2003. Notch-1 induction, a novel activity of SV40 required for growth of SV40-transformed human mesothelial cells. Oncogene **22:**81–89.
2. **Boshoff, C., T. F. Schulz, M. M. Kennedy, A. K. Graham, C. Fisher, A. Thomas, J. O. McGee, R. A. Weiss, and J. J. O'Leary.** 1995. Kaposi's sarcoma-associated herpesvirus infects endothelial and spindle cells. Nat. Med. **1:**1274–1278.
3. **Cannon, J. S., D. Ciufo, A. L. Hawkins, C. A. Griffin, M. J. Borowitz, G. S. Hayward, and R. F. Ambinder.** 2000. A new primary effusion lymphoma-derived cell line yields a highly infectious Kaposi's sarcoma herpesvirus-containing supernatant. J. Virol. **74:**10187–10193.
4. **Carroll, P. A., E. Brazeau, and M. Lagunoff.** 2004. Kaposi's sarcoma-associated herpesvirus infection of blood endothelial cells induces lymphatic differentiation. Virology **328:**7–18.
5. **Cesarman, E., Y. Chang, P. S. Moore, J. W. Said, and D. M. Knowles.** 1995. Kaposi's sarcoma-associated herpesvirus-like DNA sequences in AIDS-related body-cavity-based lymphomas. N. Engl. J. Med. **332:**1186–1191.
6. **Cesarman, E., P. S. Moore, P. H. Rao, G. Inghirami, D. M. Knowles, and Y. Chang.** 1995. In vitro establishment and characterization of two acquired immunodeficiency syndrome-related lymphoma cell lines (BC-1 and BC-2) containing Kaposi's sarcoma-associated herpesvirus-like (KSHV) DNA sequences. Blood **86:**2708–2714.
7. **Chang, H., Y. Gwack, D. Kingston, J. Souvlis, X. Liang, R. E. Means, E. Cesarman, L. Hutt-Fletcher, and J. U. Jung.** 2005. Activation of CD21 and CD23 gene expression by Kaposi's sarcoma-associated herpesvirus RTA. J. Virol. **79:**4651–4663.
8. **Chang, Y., E. Cesarman, M. S. Pessin, F. Lee, J. Culpepper, D. M. Knowles, and P. S. Moore.** 1994. Identification of herpesvirus-like DNA sequences in AIDS-associated Kaposi's sarcoma. Science **266:**1865–1869.
9. **Chiou, C. J., L. J. Poole, P. S. Kim, D. M. Ciufo, J. S. Cannon, C. M. ap Rhys, D. J. Alcendor, J. C. Zong, R. F. Ambinder, and G. S. Hayward.** 2002. Patterns of gene expression and a transactivation function exhibited by the vGCR (ORF74) chemokine receptor protein of Kaposi's sarcoma-associated herpesvirus. J. Virol. **76:**3421–3439.
10. **Ciufo, D. M., J. S. Cannon, L. J. Poole, F. Y. Wu, P. Murray, R. F. Ambinder, and G. S. Hayward.** 2001. Spindle cell conversion by Kaposi's sarcoma-associated herpesvirus: formation of colonies and plaques with mixed lytic and latent gene expression in infected primary dermal microvascular endothelial cell cultures. J. Virol. **75:**5614–5626.
11. **Coscoy, L., and D. Ganem.** 2000. Kaposi's sarcoma-associated herpesvirus encodes two proteins that block cell surface display of MHC class I chains by enhancing their endocytosis. Proc. Natl. Acad. Sci. USA **97:**8051–8056.
12. **Coscoy, L., and D. Ganem.** 2001. A viral protein that selectively downregulates ICAM-1 and B7-2 and modulates T cell costimulation. J. Clin. Investig. **107:**1599–1606.

13. **Curry, C. L., L. L. Reed, T. E. Golde, L. Miele, B. J. Nickoloff, and K. E. Foreman.** 2005. Gamma secretase inhibitor blocks Notch activation and induces apoptosis in Kaposi's sarcoma tumor cells. Oncogene **24:**6333–6344.
14. **Deng, H., M. J. Song, J. T. Chu, and R. Sun.** 2002. Transcriptional regulation of the interleukin-6 gene of human herpesvirus 8 (Kaposi's sarcoma-associated herpesvirus). J. Virol. **76:**8252–8264.
15. **Dezube, B. J., M. Zambela, D. R. Sage, J. F. Wang, and J. D. Fingeroth.** 2002. Characterization of Kaposi sarcoma-associated herpesvirus/human herpesvirus-8 infection of human vascular endothelial cells: early events. Blood **100:**888–896.
16. **Dittmer, D., M. Lagunoff, R. Renne, K. Staskus, A. Haase, and D. Ganem.** 1998. A cluster of latently expressed genes in Kaposi's sarcoma-associated herpesvirus. J. Virol. **72:**8309–8315.
17. **Dittmer, D. P.** 2003. Transcription profile of Kaposi's sarcoma-associated herpesvirus in primary Kaposi's sarcoma lesions as determined by real-time PCR arrays. Cancer Res. **63:**2010–2015.
18. **Dittmer, D. P., C. M. Gonzalez, W. Vahrson, S. M. DeWire, R. Hines-Boykin, and B. Damania.** 2005. Whole-genome transcription profiling of rhesus monkey rhadinovirus. J. Virol. **79:**8637–8650.
19. **Dumont, E., K. P. Fuchs, G. Bommer, B. Christoph, E. Kremmer, and B. Kempkes.** 2000. Neoplastic transformation by Notch is independent of transcriptional activation by RBP-J signalling. Oncogene **19:**556–561.
20. **Fakhari, F. D., and D. P. Dittmer.** 2002. Charting latency transcripts in Kaposi's sarcoma-associated herpesvirus by whole-genome real-time quantitative PCR. J. Virol. **76:**6213–6223.
21. **Gordadze, A. V., R. Peng, J. Tan, G. Liu, R. Sutton, B. Kempkes, G. W. Bornkamm, and P. D. Ling.** 2001. Notch1IC partially replaces EBNA2 function in B cells immortalized by Epstein-Barr virus. J. Virol. **75:**5899–5912.
22. **Gradoville, L., J. Gerlach, E. Grogan, D. Shedd, S. Nikiforow, C. Metroka, and G. Miller.** 2000. Kaposi's sarcoma-associated herpesvirus open reading frame 50/Rta protein activates the entire viral lytic cycle in the HH-B2 primary effusion lymphoma cell line. J. Virol. **74:**6207–6212.
23. **Gwack, Y., H. J. Baek, H. Nakamura, S. H. Lee, M. Meisterernst, R. G. Roeder, and J. U. Jung.** 2003. Principal role of TRAP/mediator and SWI/SNF complexes in Kaposi's sarcoma-associated herpesvirus RTA-mediated lytic reactivation. Mol. Cell. Biol. **23:**2055–2067.
24. **Gwack, Y., H. Byun, S. Hwang, C. Lim, and J. Choe.** 2001. CREB-binding protein and histone deacetylase regulate the transcriptional activity of Kaposi's sarcoma-associated herpesvirus open reading frame 50. J. Virol. **75:**1909–1917.
25. **Gwack, Y., S. Hwang, C. Lim, Y. S. Won, C. H. Lee, and J. Choe.** 2002. Kaposi's sarcoma-associated herpesvirus open reading frame 50 stimulates the transcriptional activity of STAT3. J. Biol. Chem. **277:**6438–6442.
26. **Hamaguchi, Y., Y. Yamamoto, H. Iwanari, S. Maruyama, T. Furukawa, N. Matsunami, and T. Honjo.** 1992. Biochemical and immunological characterization of the DNA binding protein (RBP-Jκ) to mouse Jκ recombination signal sequence. J. Biochem. (Tokyo) **112:**314–320.
27. **Hayward, G. S.** 2003. Initiation of angiogenic Kaposi's sarcoma lesions. Cancer Cell **3:**1–3.
28. **Hayward, S. D.** 2004. Viral interactions with the Notch pathway. Semin. Cancer Biol. **14:**387–396.
29. **Hsieh, J. J., and S. D. Hayward.** 1995. Masking of the CBF1/RBPJκ transcriptional repression domain by Epstein-Barr virus EBNA2. Science **268:**560–563.
30. **Hsieh, J. J., T. Henkel, P. Salmon, E. Robey, M. G. Peterson, and S. D. Hayward.** 1996. Truncated mammalian Notch1 activates CBF1/RBPJκ-repressed genes by a mechanism resembling that of Epstein-Barr virus EBNA2. Mol. Cell. Biol. **16:**952–959.
31. **Ishido, S., J. K. Choi, B. S. Lee, C. Wang, M. DeMaria, R. P. Johnson, G. B. Cohen, and J. U. Jung.** 2000. Inhibition of natural killer cell-mediated cytotoxicity by Kaposi's sarcoma-associated herpesvirus K5 protein. Immunity **13:**365–374.
32. **Ishido, S., C. Wang, B. S. Lee, G. B. Cohen, and J. U. Jung.** 2000. Downregulation of major histocompatibility complex class I molecules by Kaposi's sarcoma-associated herpesvirus K3 and K5 proteins. J. Virol. **74:**5300–5309.
33. **Jeong, J. H., R. Hines-Boykin, J. D. Ash, and D. P. Dittmer.** 2002. Tissue specificity of the Kaposi's sarcoma-associated herpesvirus latent nuclear antigen (LANA/orf73) promoter in transgenic mice. J. Virol. **76:**11024–11032.
34. **Kawaichi, M., C. Oka, S. Shibayama, A. E. Koromilas, N. Matsunami, Y. Hamaguchi, and T. Honjo.** 1992. Genomic organization of mouse Jκ recombination signal binding protein (RBP-Jκ) gene. J. Biol. Chem. **267:**4016–4022.
35. **Lagunoff, M., J. Bechtel, E. Venetsanakos, A. M. Roy, N. Abbey, B. Herndier, M. McMahon, and D. Ganem.** 2002. De novo infection and serial transmission of Kaposi's sarcoma-associated herpesvirus in cultured endothelial cells. J. Virol. **76:**2440–2448.
36. **Lan, K., D. A. Kuppers, and E. S. Robertson.** 2005. Kaposi's sarcoma-associated herpesvirus reactivation is regulated by interaction of latency-associated nuclear antigen with recombination signal sequence-binding protein Jκ, the major downstream effector of the Notch signaling pathway. J. Virol. **79:**3468–3478.
37. **Liang, Y., J. Chang, S. J. Lynch, D. M. Lukac, and D. Ganem.** 2002. The lytic switch protein of KSHV activates gene expression via functional interaction with RBP-Jκ (CSL), the target of the Notch signaling pathway. Genes Dev. **16:**1977–1989.
38. **Liang, Y., and D. Ganem.** 2003. Lytic but not latent infection by Kaposi's sarcoma-associated herpesvirus requires host CSL protein, the mediator of Notch signaling. Proc. Natl. Acad. Sci. USA **100:**8490–8495.
39. **Liang, Y., and D. Ganem.** 2004. RBP-J (CSL) is essential for activation of the K14/vGPCR promoter of Kaposi's sarcoma-associated herpesvirus by the lytic switch protein RTA. J. Virol. **78:**6818–6826.
40. **Liao, W., Y. Tang, Y. L. Kuo, B. Y. Liu, C. J. Xu, and C. Z. Giam.** 2003. Kaposi's sarcoma-associated herpesvirus/human herpesvirus 8 transcriptional activator Rta is an oligomeric DNA-binding protein that interacts with tandem arrays of phased A/T-trinucleotide motifs. J. Virol. **77:**9399–9411.
41. **Ling, P. D., and S. D. Hayward.** 1995. Contribution of conserved amino acids in mediating the interaction between EBNA2 and CBF1/RBPJκ. J. Virol. **69:**1944–1950.
42. **Lu, F. M., and S. E. Lux.** 1996. Constitutively active human Notch1 binds to the transcription factor CBF1 and stimulates transcription through a promoter containing a CBF1-responsive element. Proc. Natl. Acad. Sci. USA **93:**5663–5667.
43. **Lukac, D. M., R. Renne, J. R. Kirshner, and D. Ganem.** 1998. Reactivation of Kaposi's sarcoma-associated herpesvirus infection from latency by expression of the ORF 50 transactivator, a homolog of the EBV R protein. Virology **252:**304–312.
44. **Maillard, I., S. H. Adler, and W. S. Pear.** 2003. Notch and the immune system. Immunity **19:**781–791.
45. **Maillard, I., T. Fang, and W. S. Pear.** 2005. Regulation of lymphoid development, differentiation, and function by the Notch pathway. Annu. Rev. Immunol. **23:**945–974.
46. **Moses, A. V., K. N. Fish, R. Ruhl, P. P. Smith, J. G. Strussenberg, L. Zhu, B. Chandran, and J. A. Nelson.** 1999. Long-term infection and transformation of dermal microvascular endothelial cells by human herpesvirus 8. J. Virol. **73:**6892–6902.
47. **Nakamura, H., M. Lu, Y. Gwack, J. Souvlis, S. L. Zeichner, and J. U. Jung.** 2003. Global changes in Kaposi's sarcoma-associated virus gene expression patterns following expression of a tetracycline-inducible Rta transactivator. J. Virol. **77:**4205–4220.
48. **Okuno, T., Y. B. Jiang, K. Ueda, K. Nishimura, T. Tamura, and K. Yamanishi.** 2002. Activation of human herpesvirus 8 open reading frame K5 independent of ORF50 expression. Virus Res. **90:**77–89.
49. **Papin, J., W. Vahrson, R. Hines-Boykin, and D. P. Dittmer.** 2005. Real-time quantitative PCR analysis of viral transcription. Methods Mol. Biol. **292:**449–480.
50. **Paulson, E., C. Tran, K. Collins, and K. Fruh.** 2001. KSHV-K5 inhibits phosphorylation of the major histocompatibility complex class I cytoplasmic tail. Virology **288:**369–378.
51. **Pavlova, I., C. Y. Lin, and S. H. Speck.** 2005. Murine gammaherpesvirus 68 Rta-dependent activation of the gene 57 promoter. Virology **333:**169–179.
52. **Radtke, F., and K. Raj.** 2003. The role of Notch in tumorigenesis: oncogene or tumour suppressor? Nat. Rev. Cancer **3:**756–767.
53. **Radtke, F., A. Wilson, S. J. Mancini, and H. R. MacDonald.** 2004. Notch regulation of lymphocyte development and function. Nat. Immunol. **5:**247–253.
54. **Robertson, E. S., J. Lin, and E. Kieff.** 1996. The amino-terminal domains of Epstein-Barr virus nuclear proteins 3A, 3B, and 3C interact with RBPJκ. J. Virol. **70:**3068–3074.
55. **Sakakibara, S., K. Ueda, J. Chen, T. Okuno, and K. Yamanishi.** 2001. Octamer-binding sequence is a key element for the autoregulation of Kaposi's sarcoma-associated herpesvirus ORF50/Lyta gene expression. J. Virol. **75:**6894–6900.
56. **Singer, P. A., and A. R. Williamson.** 1980. Cell surface immunoglobulin mu and gamma chains of human lymphoid cells are of higher apparent molecular weight than their secreted counterparts. Eur. J. Immunol. **10:**180–186.
57. **Song, M. J., X. Li, H. J. Brown, and R. Sun.** 2002. Characterization of interactions between RTA and the promoter of polyadenylated nuclear RNA in Kaposi's sarcoma-associated herpesvirus/human herpesvirus 8. J. Virol. **76:**5000–5013.
58. **Staudt, M. R., Y. Kanan, J. H. Jeong, J. F. Papin, R. Hines-Boykin, and D. P. Dittmer.** 2004. The tumor microenvironment controls primary effusion lymphoma growth in vivo. Cancer Res. **64:**4790–4799.
59. **Strobl, L. J., H. Hofelmayr, G. Marschall, M. Brielmeier, G. W. Bornkamm, and U. Zimber-Strobl.** 2000. Activated Notch1 modulates gene expression in B cells similarly to Epstein-Barr viral nuclear antigen 2. J. Virol. **74:**1727–1735.
60. **Sun, R., S. F. Lin, L. Gradoville, Y. Yuan, F. Zhu, and G. Miller.** 1998. A viral gene that activates lytic cycle expression of Kaposi's sarcoma-associated herpesvirus. Proc. Natl. Acad. Sci. USA **95:**10866–10871.
61. **Tani, S., H. Kurooka, T. Aoki, N. Hashimoto, and T. Honjo.** 2001. The N- and C-terminal regions of RBP-J interact with the ankyrin repeats of Notch1 RAMIC to activate transcription. Nucleic Acids Res. **29:**1373–1380.
62. **Tomescu, C., W. K. Law, and D. H. Kedes.** 2003. Surface downregulation of major histocompatibility complex class I, PE-CAM, and ICAM-1 following

de novo infection of endothelial cells with Kaposi's sarcoma-associated herpesvirus. J. Virol. **77:**9669–9684.

63. **Veeraraghavalu, K., M. Pett, R. V. Kumar, P. Nair, A. Rangarajan, M. A. Stanley, and S. Krishna.** 2004. Papillomavirus-mediated neoplastic progression is associated with reciprocal changes in Jagged1 and Manic Fringe expression linked to Notch activation. J. Virol. **78:**8687–8700.
64. **Wang, S., S. Liu, M. H. Wu, Y. Geng, and C. Wood.** 2001. Identification of a cellular protein that interacts and synergizes with the RTA (ORF50) protein of Kaposi's sarcoma-associated herpesvirus in transcriptional activation. J. Virol. **75:**11961–11973.
65. **Zhou, F. C., Y. J. Zhang, J. H. Deng, X. P. Wang, H. Y. Pan, E. Hettler, and S. J. Gao.** 2002. Efficient infection by a recombinant Kaposi's sarcoma-associated herpesvirus cloned in a bacterial artificial chromosome: application for genetic analysis. J. Virol. **76:**6185–6196.
66. **Zimber-Strobl, U., and L. J. Strobl.** 2001. EBNA2 and Notch signalling in Epstein-Barr virus mediated immortalization of B lymphocytes. Semin. Cancer Biol. **11:**423–434.